TECH. MEMO AERO 2164 | UNLIMITED | TECH. MEMO AERO 2164

ROYAL AEROSPACE ESTABLISHMENT

THE AERODYNAMIC CHARACTERISTICS OF POWER-LAW BODIES IN CONTINUUM AND TRANSITIONAL HYPERSONIC FLOW

by

M. F. Westby
J. D. Regan

August 1989

Procurement Executive, Ministry of Defence
Farnborough, Hampshire

UNLIMITED

CONDITIONS OF RELEASE

0053550 BR-111667

.... U

.... Y

Reports quoted are not necessarily available to members of the public or to commercial organisations.

UNLIMITED

ROYAL AEROSPACE ESTABLISHMENT

Technical Memorandum Aero 2164

Received for printing 3 August 1989

THE AERODYNAMIC CHARACTERISTICS OF POWER-LAW BODIES IN CONTINUUM AND TRANSITIONAL HYPERSONIC FLOW

by

M. F. Westby

J. D. Regan

SUMMARY

This Memorandum describes experimental studies carried out at the RAE in the Low Density Tunnel and Gun Tunnel to determine the aerodynamic characteristics of a series of power-law bodies of constant fineness ratio over a Reynolds number range covering both continuum and transitional rarefied flow. The tests were carried out at Mach numbers of 10 in the Low Density Tunnel and 12.8 in the Gun Tunnel at angles of incidence up to 30°.

Paper presented at the International Conference on Hypersonic Aerodynamics, University of Manchester, 4 to 6 September 1989.

UNLIMITED

LIST OF CONTENTS

		Page
1	INTRODUCTION	3
2	DESCRIPTION OF FACILITIES AND TESTS	3
3	DESCRIPTION OF MODELS	5
4	DISCUSSION OF RESULTS	6
	4.1 Axial force coefficient	6
	4.2 Normal force coefficient	8
	4.3 Centre of pressure position	9
5	CONCLUSIONS	10
List of symbols		11
References		13
Illustrations		Figures 1-10
Report documentation page		inside back cover

1 INTRODUCTION

In recent years there has been considerable interest in the aerodynamic characteristics of slender blunted cones moving through the atmosphere at hypersonic velocities. Much work has been done in this field and has shown that slender blunted conical bodies have desirable hypersonic aerodynamic characteristics. However, the slenderness of the bodies means that they have a small internal volume for given overall dimensions thus limiting their practical usefulness. Power-law bodies of revolution may be an alternative configuration to blunted cones for certain applications, as, for a given fineness ratio, a power-law body has a greater internal volume than a blunted cone.

A further attribute of the power-law body is that various theories predict that a power-law body represents the minimum drag case at hypersonic speeds. However, with the exception of Regan[1] and Peckham[2], few experimental studies have been carried out on power-law bodies of what might be termed 'practical' configurations. Most of the experimental studies have concentrated on the flow around very slender bodies ($l/d \geqslant 10$) and few have measured aerodynamic performance characteristics (*ie* force coefficients). In addition, to the authors' knowledge, no studies have been undertaken in the transitional rarefied flow regime, that region between continuum and free-molecular flow where viscous effects become increasingly significant.

This Memorandum describes two investigations undertaken to study the aerodynamic characteristics of a series of power-law bodies. The experiments were designed to gain some understanding of the effect of varying configuration and Reynolds number on the performance of a family of slender axisymmetric bodies, including two configurations which have been predicted to be minimum drag bodies at hypersonic speeds.

The first investigation was undertaken in continuum flow in the RAE Gun Tunnel. Longitudinal (or pitch plane) aerodynamic characteristics were measured at a Mach number of 12.8 over an incidence range of zero to 20°. The second investigation was undertaken in transitional rarefied flow at a Mach number of 9.84 in the RAE Low Density Tunnel. Longitudinal aerodynamic characteristics were measured at up to 30° incidence over a range of Reynolds number.

2 DESCRIPTION OF FACILITIES AND TESTS

The RAE Low Density Tunnel is a continuously running facility that uses nitrogen as its working fluid. For the tests described in this Memorandum, the free-stream Mach number was held constant at 9.84, whilst the stagnation pressure

varied between 1.8 and 2.1 bars; stagnation temperatures ranged from 1170 to 1660K. By running the tunnel at these various stagnation conditions, three different values of freestream Reynolds number were achieved. In addition, two different sizes of model were tested giving a total of six Reynolds numbers, based on model base diameter. These varied between 1936 and 6200. At these Reynolds numbers significant non-continuum effects were present in all the tests.

In contrast to the Low Density Tunnel, the RAE Gun Tunnel is a short duration facility, with a run time of the order of 50 ms, using nitrogen as a test gas. The tests described were performed at a free-stream Mach number of 12.8. The tunnel was operated at a nominal stagnation pressure of 150 bars and a stagnation temperature of 1100K, just sufficient to avoid liquefaction in the working section. Only one size of model was tested in the Gun Tunnel, resulting in a Reynolds number based on model base diameter of 350000. This ensured that all of the tests were carried out well within the continuum regime. On a model of the size tested, the boundary layer was likely to be laminar along the whole length of the body at the Gun Tunnel test conditions.

In the Low Density Tunnel the models were suspended from a three component electro-magnetic balance (Fig 1a) to measure the value of axial force, normal force and pitching moment. The balance operates on the null principle and can measure loads of up to 1.0 N axial and normal force and 0.1 Nm pitching moment. It is mounted on the roof of the evacuated working section and carefully shielded from the high temperature free jet to prevent any measurement errors due to heating effects.

Other possible sources of error were sting and shroud interference. It is generally accepted for continuum flow that the sting diameter must be less than 30% of the model base diameter for the results to be interference free[3]. The stings used in the Low Density Tunnel were less than 16% of the base diameter of the smaller models, so sting interference effects should hopefully be negligible in this rarefied flow. Shroud interference occurs if the model is mounted too close to the vertical-sting shroud. The flow around the shroud interacts with the model base flow, changing the pressure field and hence the aerodynamic forces. Tests have been carried out previously to determine the minimum clearance required to avoid shroud interference and the resulting guidelines have been followed in these tests.

The force balance used in the Gun Tunnel was an internally mounted, conventionally designed, miniature three-component strain gauge force balance operating in the pitch plane. Because of the small forces acting on the model,

semiconductor strain gauges, which are some 50 times more sensitive than conventional types, were used as bridge elements at the balance gauge stations. Thus, relatively small aerodynamic forces on the models could be measured with an acceptable degree of accuracy. Semi-conductor gauges are acceptable for the very short run time of the Gun Tunnel, although they are prone to drift with time and are very sensitive to temperature changes.

The sting diameter was around 27% of the model base diameter. Hence the results can be considered relatively free from sting interference effects. Shroud interference is absent in the Gun Tunnel as the horizontal sting is attached directly to a small quadrant type incidence gear in the centre of the working section (Fig 1b). This quadrant is both small enough and far enough away from the model for any interference problems to be avoided.

Both the Low Density Tunnel and the Gun Tunnel are open jet type wind tunnels. The Low Density Tunnel has a jet core diameter of about 200 mm. This meant that the maximum incidence that could be achieved with the larger models was 30°. At higher angles the models would partially block the tunnel, resulting in measurement errors. The smaller models used in the Low Density Tunnel were tested over the same range of incidence as the larger ones. The Gun Tunnel has a core diameter in excess of 200 mm, allowing incidences of up to 35° to be tested. However, in this series of experiments, the models were only tested at incidences of up to 20°.

3 DESCRIPTION OF MODELS

A power-law body is a body of revolution formed by rotating the generator:

$$y = \frac{d}{2}\left(\frac{x}{l}\right)^n ,$$

about the x-axis. y is the local radius of the body at a distance x from the nose, while d is the base diameter and l, the overall length. This type of configuration is of interest as various theories have predicted a power-law body to be the minimum drag axisymmetric shape for hypersonic speeds. However, there is some dispute as to what the exponent is, for the lowest drag. Cole[4], using hypersonic small disturbance theory, came to the conclusion that a power-law body with an exponent of 2/3 was the minimum drag configuration, whereas Eggers[5], using Newtonian theory, modified to take account of centrifugal effects, found that an exponent of 3/4 gave the minimum drag solution.

Therefore, four sets of models were tested in both the Low Density Tunnel and the Gun Tunnel (Fig 2). The four sets were bodies with power-law exponents of 1/2 (a parabola of revolution), 2/3, 3/4 and 1 (a pointed cone). The 2/3 and 3/4 configurations would test the relative merits of Cole's and Eggers' theories, whilst the cone would provide a reference and the parabola of revolution would show the effect of gross changes in configuration.

Two models of each type were constructed for testing in the Low Density Tunnel. The smaller of each type had a base diameter of 30.63 mm, whilst the larger had a base diameter of 50 mm. One model of each type was constructed for testing in the Gun Tunnel, each having a base diameter of 63.5 mm. All models constructed had a fineness ratio of 2, that is their overall length was twice their base diameter. This ratio was chosen as being the same as that tested by Peckham[2] in his earlier work. It has other advantages in that the bodies are blunt enough for significant differences in body shape to be apparent, yet they should still be slender enough for small disturbance theory to be applicable.

4 DISCUSSION OF RESULTS

Figs 3, 7 and 9 show the variation with incidence of axial force coefficient, normal force coefficient and centre of pressure position respectively. Data are presented for all seven values of Reynolds number tested in the two facilities and for the two extremes of body configuration ($n = 1/2$ and $n = 1$). The individually plotted symbols represent experimental data; the two solid lines above and below the experimental results in these figures are the inviscid (lower line) and free-molecular (upper line) limits. The corresponding plots for $n = 2/3$ and $n = 3/4$ are not presented due to their similarity to those in the figures. The inviscid limit was evaluated using modified Newtonian theory, and the free-molecular limit using impact theory with various assumptions being made about flow velocity, wall temperature and accommodation coefficient[6].

Figs 4, 8 and 10 show the change of the three characteristics of the bodies with incidence for all of the power-law exponents. Data are presented at three Reynolds numbers spanning the range of tests carried out in rarefied flow and for the tests carried out in continuum flow in the Gun Tunnel. Note that the ordinate scales of Fig 4 are different to those if Fig 3 and that the scales in Fig 4 cover different ranges of C_A to allow maximum clarity.

4.1 Axial force coefficient

From Fig 3 it can be seen that throughout the incidence range tested, the axial force coefficient increases with decreasing Reynolds number. All of the

data lie nearer to the continuum limit than the free-molecular limit. This is to be expected, as the data from the Gun Tunnel (Re = 350000) is well into the continuum flow regime and the data from the Low Density Tunnel (Re $\leqslant$ 6200) lies in the transitional rarefied flow regime, but at the continuum end of the range.

The trends observed in these data are similar to those seen in previous work on slender blunted cones in rarefied flow[7]. The rise in axial force coefficient with decreasing Reynolds number is caused by the increasing influence of interaction processes between the rarefied flow and the surface of the body, leading to the formation of a relatively thick boundary layer.

Fig 4 shows the variation of axial force coefficient with incidence and exponent. It can be seen that in continuum flow, body shape has a clear, but small influence on the axial force coefficient. Throughout the incidence range the $n = 3/4$ body has the lowest value of C_A. $n = 2/3$ has slightly higher values, with $n = 1$ and $n = 1/2$ being higher still by a noticeable margin.

This trend cannot be seen for any of the rarefied flow results. It would appear that in general (taking into account all measurements made in rarefied flow, not just the data presented), $n = 1$ has the highest axial force coefficient, but the body having the lowest C_A is not clear from any of the results. However, no firm conclusions can be drawn from these results as the variations in C_A observed are of the same order of magnitude as the resolution of the force balance used in the Low Density Tunnel. In any case, it can be seen from Figs 3 and 4 that any change in the axial force coefficient due to body shape in rarefied flow is negligible compared to the increase in C_A with decreasing Reynolds number.

Another point to note from Fig 3 is that all of the results for a given Reynolds number lie in approximately the same positions with respect to the continuum and free-molecular limits. Because of this, the results for all four configurations can be collapsed by using the function:

$$\phi = \frac{C_A - C_{Ai}}{C_{Afm} - C_{Ai}} .$$

Fig 5 shows the zero incidence values of ϕ for all four bodies plotted against Knudsen number.

The Knudsen number is the ratio of the ambient mean free path of the gas molecules to some reference length (in this case, the body base diameter).

It provides a useful guide to the degree of rarefaction of the flow. Note that all of the resu lie close together with the exception of $n = 1/2$ which is slightly lower. ..il of these results can be linked using a bridging function with the equation:

$$\phi(Kn) = \frac{(Kn + 0.001655)(Kn + 0.0000149)}{(Kn + 0.03309)(Kn + 0.0000736)} ,$$

(shown as the solid line on Fig 5). Thus the magnitude of the axial force coefficient may be predicted approximately through the transitional rarefied flow regime if the values of C_{Ai} and C_{Afm} are known.

An attempt was made to compare the relative performance of the bodies when body geometry was taken into account. It was felt that the best way of doing this was to factor the value of zero-incidence axial force coefficient against body volume. Thus, Fig 6 is a comparison of C_A with C_A divided by the volume of the body in question, relative to the volume of the sharp cone (results are for continuum flow only). This shows that whilst the minimum drag case is the $n = 3/4$ body, the $n = 2/3$ body has the lowest value of drag per unit volume of any of the configurations tested.

4.2 Normal force coefficient

Fig 7 shows plots of normal force coefficient for the same flow conditions and values of the exponent as those shown in Fig 3. As with C_A, it can be seen that the normal force increases as the value of Reynolds number is reduced. However, the increase in C_N is proportionally far less than the rise in C_A for a given change in Reynolds number.

It can also be seen that, unlike the values of axial force coefficient, the values of C_N do not always lie nearer to the continuum limit than the free-molecular limit. The data for the body with $n = 1/2$ lie closest to the continuum limit. However, as the bluntness of the bodies is reduced the values of C_N move towards the free-molecular limit until when $n = 1$ the values of C_N for the lowest Reynolds number lie on or around the free-molecular limit. Thus, bridging functions of the same form as those used for axial force coefficients cannot be used to predict the magnitude of the normal force coefficient. This effect is probably due to assumptions used in the calculation of the free-molecular normal force coefficient (for instance body wall temperature or accommodation coefficient) being slightly in error.

Fig 8 shows the variations in normal force coefficient with exponent at the same Reynolds numbers as Fig 4. As with axial force coefficient, it can be seen that body shape has little influence on the magnitude of C_N in rarefied flow, Reynolds number being the dominant effect. However, at the highest angles of incidence tested the trend seems to be that C_N increases with increasing bluntness (*ie* from $n = 1$ to $n = 1/2$). This is probably due to the blunter bodies being physically larger than the more slender ones and so having larger surface areas for the pressure and shear forces to act upon.

A departure from the trend was seen in continuum flow. At high angles of incidence, apart from the parabola of revolution, the trend was the same as for the rarefied flow data, with the two intermediate bodies producing higher values of C_N than the cone. However, the parabola of revolution had a lower value of C_N than any of the others. The reason for this anomaly is not clear, but it could be that the pressure coefficient around the nose is reduced due to centrifugal effects around the highly curved nose. These would probably only be seen on the parabola of revolution as the nose curvature of the two intermediate ($n = 2/3$ and $n = 3/4$) bodies is small compared with the $n = 1/2$ body.

4.3 Centre of pressure position

The variation of the centre of pressure position (X_{cp}/l) with incidence and Reynolds number is shown in Fig 9. X_{cp}/l is calculated from the ratio of pitching moment about the nose of the body to normal force. The pitching moment is the most difficult characteristic to measure, as any small changes in the axial position of the body when rigging different models in the wind tunnel will introduce errors into the results. This, coupled with the fact that X_{cp}/l is derived from the ratio of two measured characteristics, both having zero incidence, means that its accuracy is less than that of the axial and normal force coefficients. For this reason, no data points have been plotted for angles of incidence less than 5° and scatter is present in the data up to about 15°.

From the figure it can be seen that Reynolds number has very little effect on the position of the centre of pressure. No trends are visible in the data as the magnitude of any changes due to Reynolds number are less than the magnitude of the errors. All of the data lie on, or very close to the Newtonian predictions (the lower solid line on the figure).

Fig 10 shows the movement of the centre of pressure position with varying body shape. These are the complete opposite of the results for C_A and C_N. Axial and normal forces were mainly affected by Reynolds number in rarefied flow,

with body shape having little discernable influence. However, the centre of pressure position is affected markedly by configuration, whilst Reynolds number has little or no influence. At all Reynolds numbers the centre of pressure shows significant forward movement with increasing bluntness. This is intuitively consistent with geometry, namely that, for a given value of fineness ratio, it moves towards the nose as the exponent decreases.

5 CONCLUSIONS

(1) The dominant influence on the magnitudes of the axial and normal force coefficients is Reynolds number. Body shape has a small influence on axial force coefficient in continuum flow. It also changes the magnitude of the normal force coefficient slightly in both continuum and rarefied flow. However, its influence is small compared with that of Reynolds number.

(2) The position of the centre of pressure is largely governed by body shape. For a given shape there is little movement in X_{cp} throughout the Reynolds number range tested. However, for a given value of Reynolds number, there is considerable movement of the centre of pressure position with changing values of the power-law exponent.

(3) In continuum flow it appears that a power-law body with the exponent equal to 3/4 is the configuration with the lowest drag. In rarefied flow it has not been possible to determine which configuration has the lowest value of axial force coefficient, nor whether the value of n for minimum drag is constant throughout the Reynolds number range.

(4) In continuum flow the body with the lowest drag per unit volume tested was the $n = 2/3$ body. Thus it seems that a body with slightly more blunting than the minimum drag body would make the most practical configuration from the load carrying point of view.

LIST OF SYMBOLS

A	base area, $\pi d^2/4$
C_A	axial force coefficient, $F/q_\infty A$
C_N	normal force coefficient, $N/q_\infty A$
d	base diameter of body
F	measured axial force
$Kn_{\infty,d}$	Knudsen number, $\lambda_\infty/d (= 1.26\gamma^{\frac{1}{2}} M_\infty/Re_{\infty,d}$
l	overall body length
M	Mach number
n	power-law exponent
N	measured normal force
q_∞	dynamic pressure, $\frac{1}{2}\rho_\infty U^2_\infty$
$Re_{\infty,d}$	Reynolds number, $\rho_\infty U_\infty d/\mu_\infty$ (sometimes written as Re)
S	surface area of body (not including base area)
U	velocity
V	internal volume of body
x	axial coordinate, measured from body nose
X_{cp}	position of centre of pressure aft of nose
y	radial coordinate, measured from body axis
α	angle of incidence
γ	ratio of specific heats
λ_∞	ambient mean free path of gas molecule
μ	viscosity
ρ	density
ϕ	$(C_A - C_{Ai})/(C_{Afm} - C_{Ai})$
$\phi(Kn)$	bridging function

LIST OF SYMBOLS (concluded)

Subscripts

cone	value for pointed cone (n = 1)
fm	free molecular value
i	inviscid value
∞	freestream value

REFERENCES

No.	Author	Title, etc
1	J.D. Regan M.R. Lynn	The drag and static stability of a series of power-law bodies at a Mach number of 12.8. RAE Technical Memorandum Aero 2054 (1985)
2	D.H. Peckham	Measurements of pressure distribution and shock wave shape on power-law bodies at a Mach number of 6.85. RAE Technical Report 65075 (1965)
3	J. Don Gray	Summary report on aerodynamic characteristics of standard models HB-1 and HB-2. AEDC-TR-64-137 (1964)
4	J.D. Cole	Newtonian flow theory for slender bodies. *J. Aero. Sci.*, 24(6), p 448-455, June (1957)
5	A.J. Eggers M.M. Resnikoff D.H. Dennis	Bodies of revolution having minimum drag at high supersonic speeds. NACA Report 1306 (1957)
6	S. Daley	Private communication (1989)
7	T.J. Rhys-Jones	The drag of slender axisymmetric cones in rarefied hypersonic flow. AGARD Symposium on Aerodynamics of Hypersonic Lifting Vehicles, Bristol (1987)

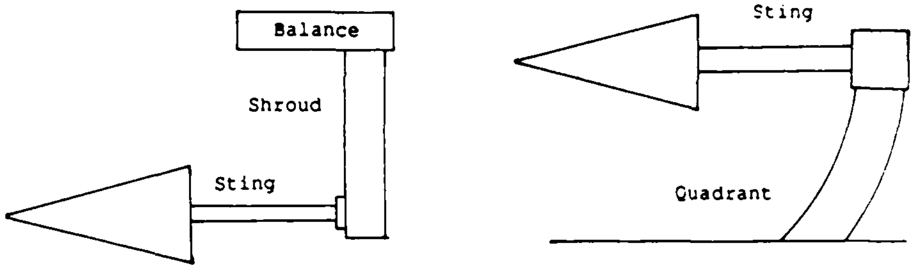

(a) low density tunnel

(b) gun tunnel

Fig 1 Details of model mountings

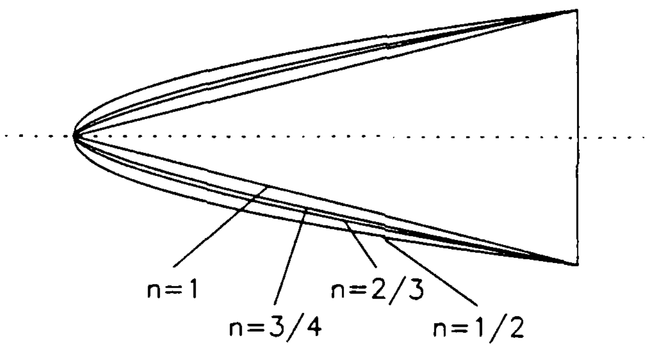

Length (mm)	Base diameter (mm)	Tunnel tested in
61.26	30.63	Low density tunnel
100.00	50.00	Low density tunnel
127.00	63.50	Gun tunnel

n	$\frac{V}{V_{cone}}$	$\frac{S}{S_{cone}}$
$\frac{1}{2}$	1.500	1.333
$\frac{2}{3}$	1.286	1.200
$\frac{3}{4}$	1.200	1.143
1	1.000	1.000

Fig 2 Configuration and dimensions of models tested

Fig 3

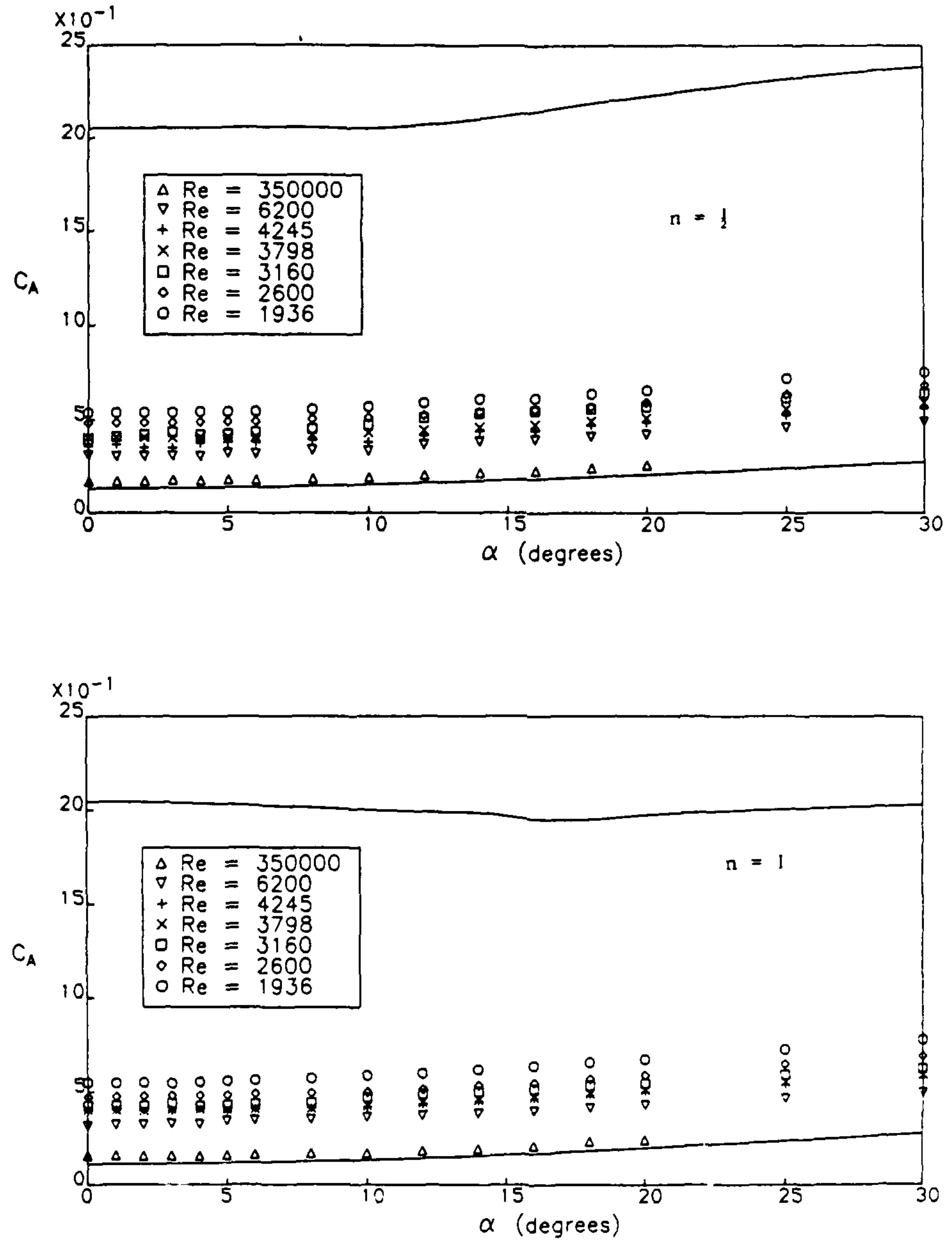

Fig 3 Plots of axial force coefficient against angle of incidence for similar geometries

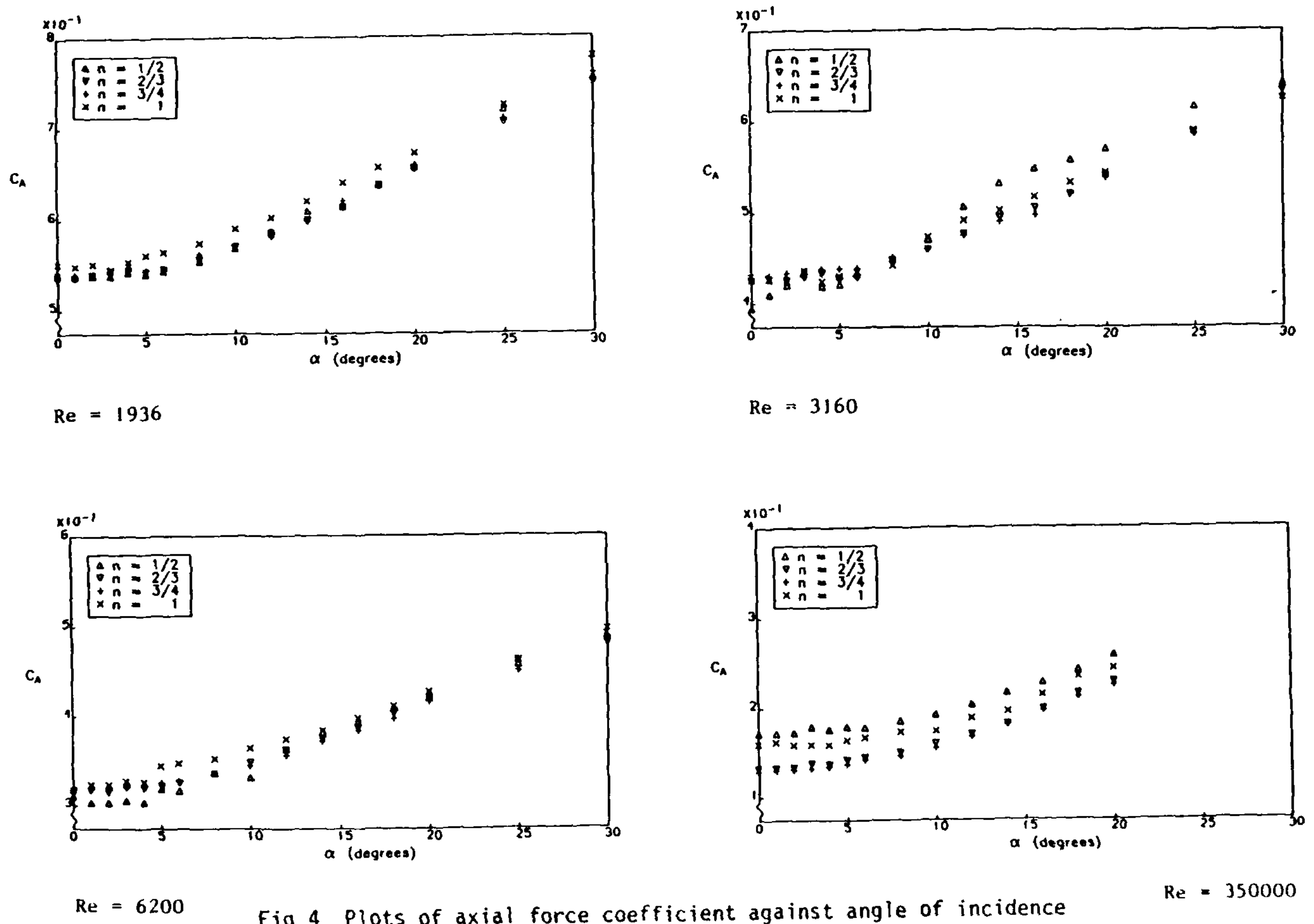

Fig 4 Plots of axial force coefficient against angle of incidence over a range of Reynolds numbers

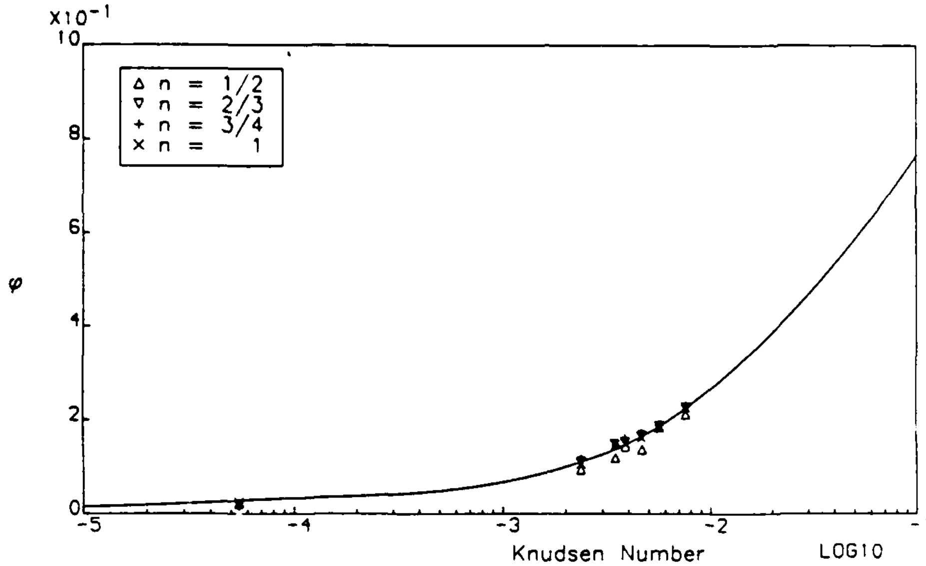

Fig 5 Comparison of zero-incidence axial force data with bridging function

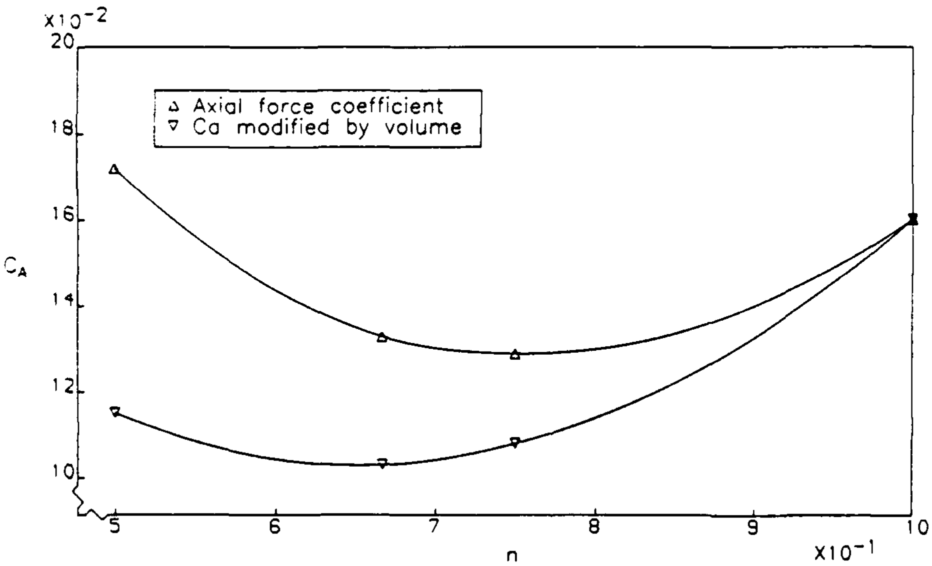

Fig 6 Plot of zero-incidence axial force coefficient modified to take account of body volume against power-law exponent. Data for continuum flow

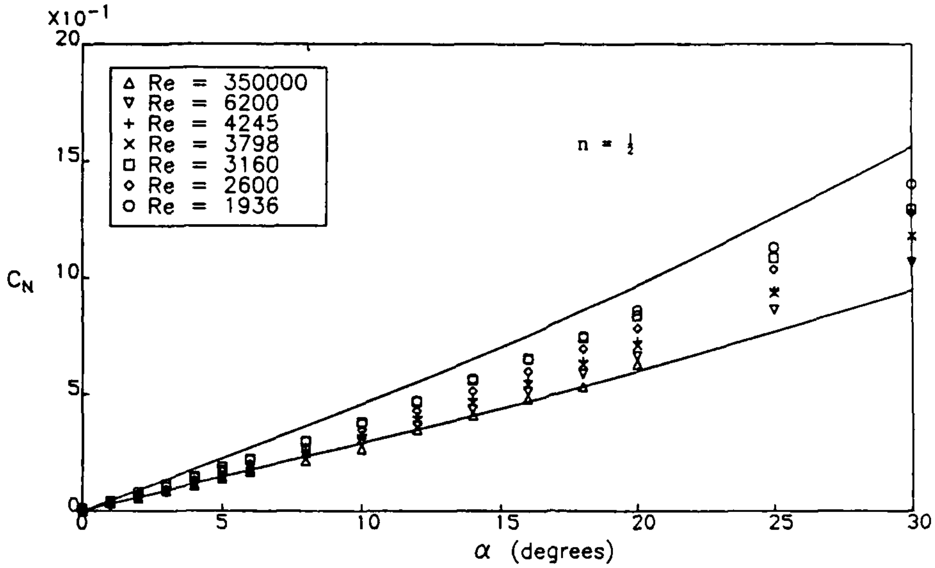

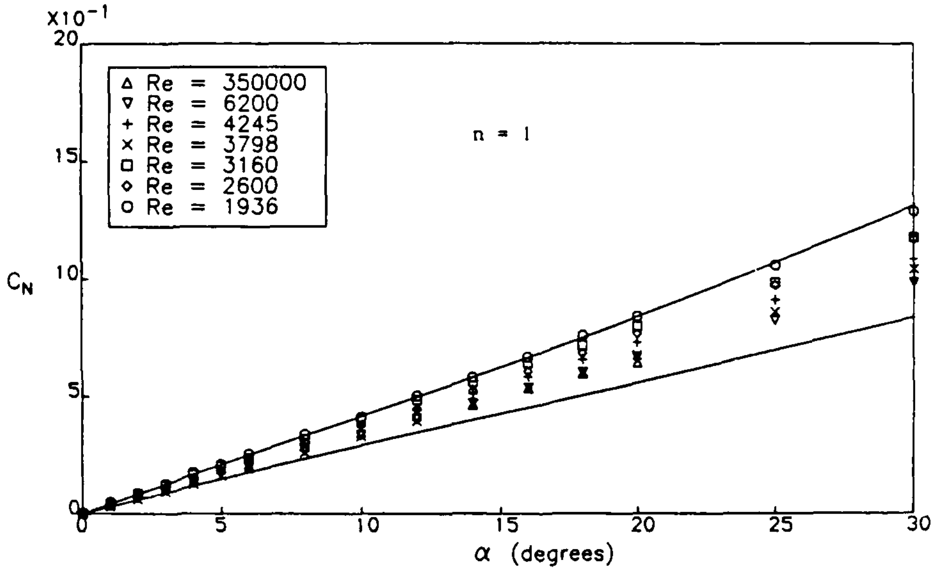

Fig 7 Plots of normal force coefficient against angle of incidence for similar geometries

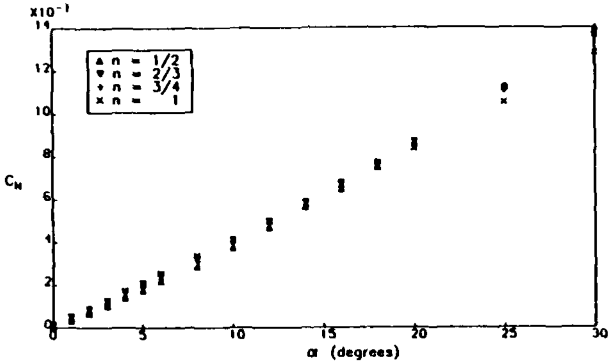

Re = 1936

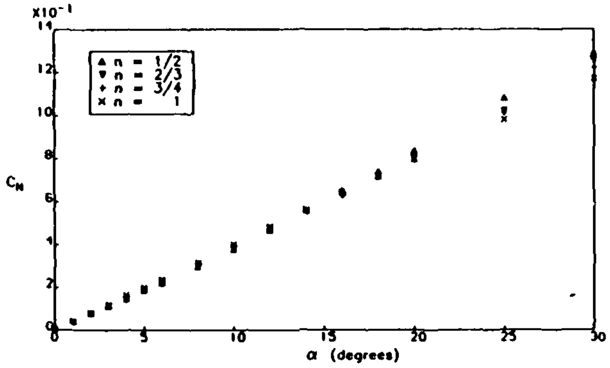

Re = 3160

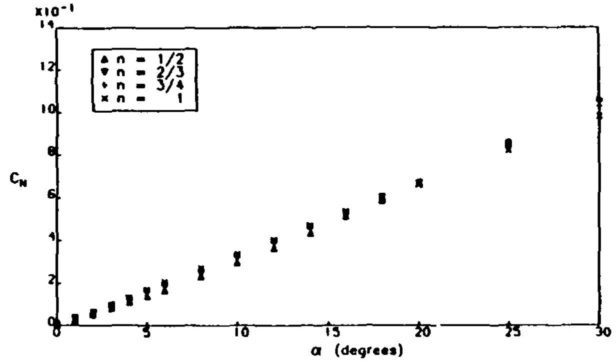

Re = 6200

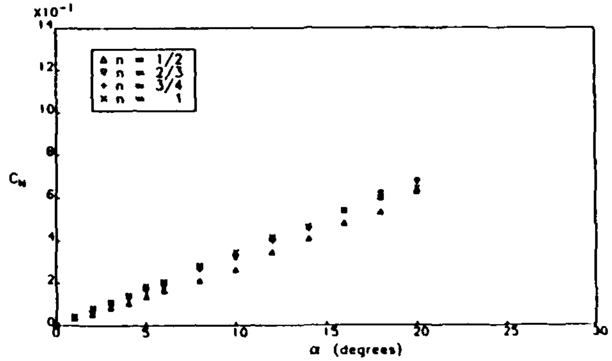

Re = 350000

Fig 8 Plots of normal force coefficient against angle of incidence over a range of Reynolds numbers

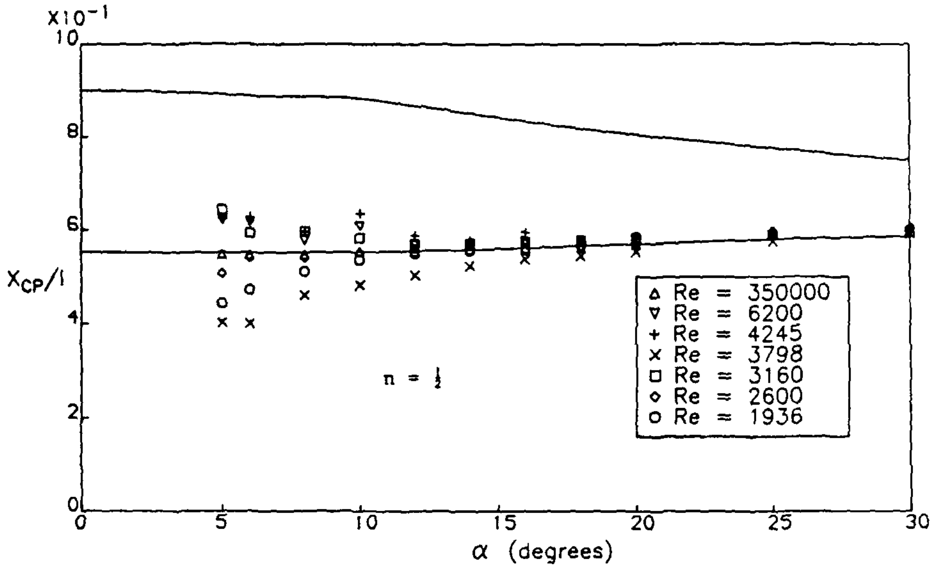

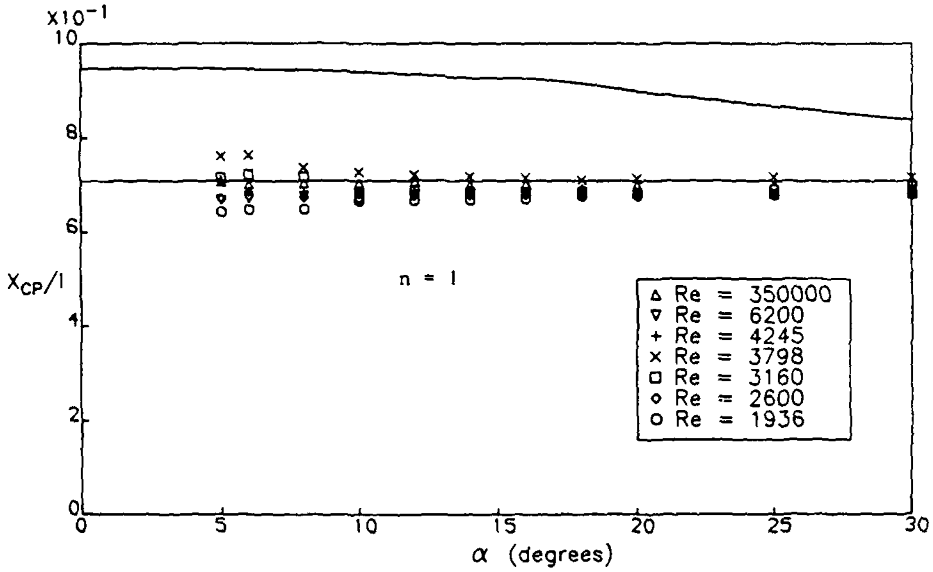

Fig 9 Change of centre of pressure position with angle of incidence for similar geometries

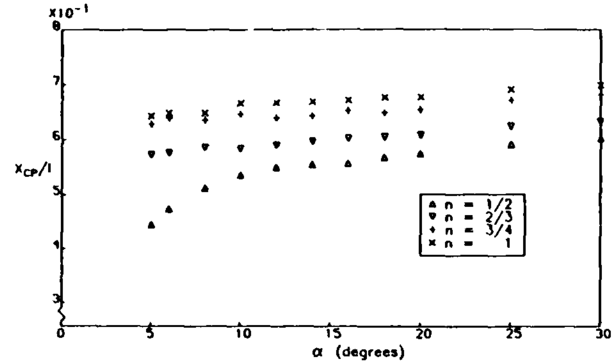

Re = 1936

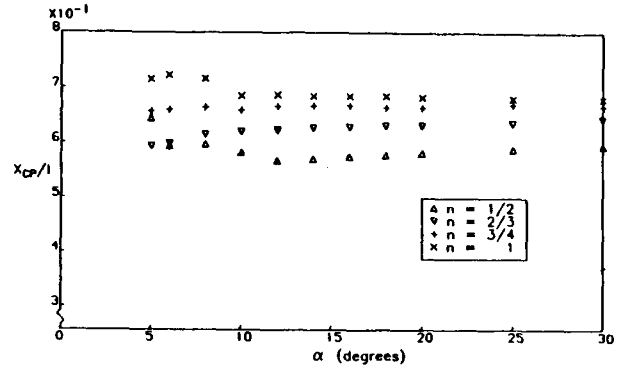

Re = 3160

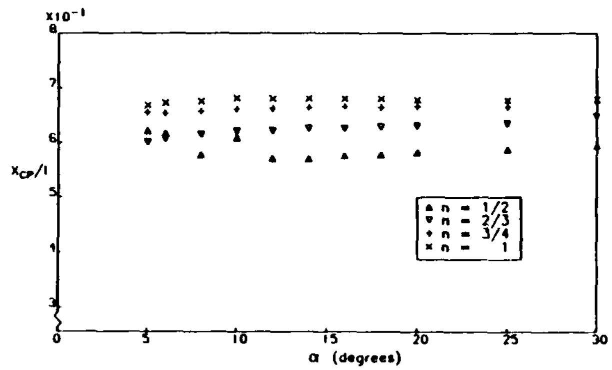

Re = 6200

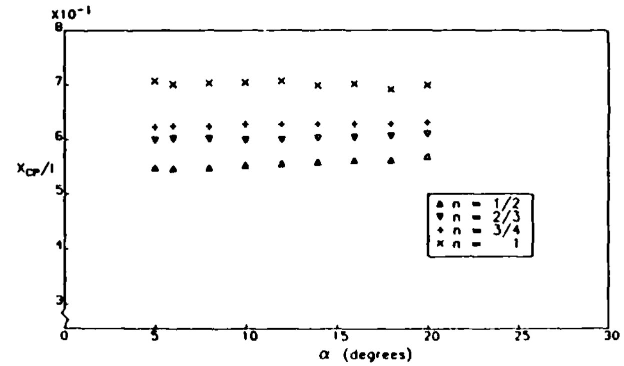

Re = 350000

Fig 10 Change of centre of pressure position with angle of incidence over a range of Reynolds numbers

REPORT DOCUMENTATION PAGE

Overall security classification of this page

UNLIMITED

As far as possible this page should contain only unclassified information. If it is necessary to enter classified information, the box above must be marked to indicate the classification, e.g. Restricted, Confidential or Secret.

1. DRIC Reference (to be added by DRIC)	2. Originator's Reference	3. Agency Reference	4. Report Security Classification/Marking
	RAE TM Aero 2164		UNLIMITED

5. DRIC Code for Originator	6. Originator (Corporate Author) Name and Location
7673000W	Royal Aerospace Establishment, Farnborough, Hants, UK.
5a. Sponsoring Agency's Code	6a. Sponsoring Agency (Contract Authority) Name and Location

7. Title The aerodynamic characteristics of power-law bodies in continuum and transitional hypersonic flow

7a. (For Translations) Title in Foreign Language

7b. (For Conference Papers) Title, Place and Date of Conference
International Conference on Hypersonic Aerodynamics, University of Manchester, 4 to 6 September 1989

8. Author 1. Surname, Initials	9a. Author 2	9b. Authors 3, 4	10. Date	Pages	Refs.
Westby, M.F.	Regan, J.D.		August 1989	22	7

11. Contract Number	12. Period	13. Project	14. Other Reference Nos.

15. Distribution statement
(a) Controlled by – Head of Aerodynamics Department, RAE
(b) Special limitations (if any) –
If it is intended that a copy of this document shall be released overseas refer to RAE Leaflet No.3 to Supplement 6 of MOD Manual 4.

16. Descriptors (Keywords) (Descriptors marked * are selected from TEST)

Hypersonic flow*; Wind tunnels*; Rarefied gases*; Slender bodies; (KT)

17. Abstract

This Memorandum describes experimental studies carried out at the RAE in the Low Density Tunnel and Gun Tunnel to determine the aerodynamic characteristics of a series of power-law bodies of constant fineness ratio over a Reynolds number range covering both continuum and transitional rarefied flow. The tests were carried out at Mach numbers of 10 in the Low Density Tunnel and 12.8 in the Gun Tunnel at angles of incidence up to 30°. degrees Keywords;

F5906/1

RAE Form A143 (revised October 1980)